EXACT SOLUTION OF FINITE GEOMETRY COMPOSITE PANELS UNDER TRANSIENT SURFACE LOADING

by

Todd Anderson

A Thesis Submitted to the Faculty of the

DEPARTMENT OF AEROSPACE AND MECHANICAL ENGINEERING

In Partial Fulfillment of the Requirements
For the Degree of

MASTER OF SCIENCE
WITH A MAJOR IN MECHANICAL ENGINEERING

In the Graduate College

THE UNIVERSITY OF ARIZONA

1995

STATEMENT BY AUTHOR

This thesis has been submitted in partial fulfillment of requirements for an advanced degree at The University of Arizona and is deposited in the University Library to be made available to borrowers under rules of the Library.

Brief quotations from this thesis are allowable without special permission, provided that accurate acknowledgment of source is made. Requests for permission for extended quotation from or reproduction of this manuscript in whole or in part may be granted by the head of the major department or the Dean of the Graduate College when in his or her judgment the proposed use of the material is in the interests of scholarship. In all other instances, however, permission must be obtained from the author.

Signed: Todd Anderson

APPROVAL BY THESIS DIRECTOR

This thesis has been approved on the date shown below:

Erdogan Madenci

Erdogan Madenci
Associate Professor of Mechanical Engineering

7-21-1995

Date

TABLE OF CONTENTS

LIST OF FIGURES

LIST OF FIGURES - *Continued*

LIST OF TABLES

ABSTRACT

The exact three-dimensional transient solution of a multi-layer orthotropic panel subjected to transverse loading is presented. The finite geometry panel, supported by rollers, is subjected to an arbitrarily distributed surface load. Governing equations derived from Reissner's functional are solved by applying Fourier or Laplace transformation in time and enforcing the continuity of traction and displacement components between the adjacent layers. Material damping is incorporated into the analysis through complex material constants. The accuracy of the present analysis is established by considering a thick and thin laminate under quasi-static and transient loading, respectively. The solution of the static analysis is compared with a known exact solution and the transient analysis is compared with a finite element analysis. Transient responses of a thick laminate and a composite sandwich panel are also investigated. Material damping is found to significantly affect the transient stress and displacement fields of a laminate.

1. INTRODUCTION

Understanding the impact damage characteristics of laminates and composite sandwich panels becomes imperative as their use increases in the construction of primary aircraft components. Sandwich panels are fabricated by bonding thin laminates (face sheets) on the outer surfaces of a light weight shear-carrying honeycomb or foam core material. Both the laminate and sandwich panels are very susceptible to low velocity (projectile velocity less than 150 ft/sec) impact such as dropped-tools, runway stones and tire blowout debris.

Although visual examination of the impacted surface reveals very little damage, most of the degradation occurs internally near the back face sheet. With a sandwich panel, damage in the form of a shallow dent, visible near the impact area is due to core crushing. Associated with the dent is a delamination at the interface between the face sheet and the core. The physical characteristics of internal damage caused by impact in composite laminates or sandwich panels can be found in Starnes and Williams (1984) and Nettles et al. (1990), respectively. Even at relatively low impact speeds, destructive and non-destructive-evaluation methods indicate the primary damage mode involves interlaminar delaminations resulting in a significant loss of bending stiffness.

Several mechanisms may participate in creating the local impact damage. During the impact event, a transient compressive normal stress is initiated and propagates through the panel. The compressive stress wave reflects from the back surface of the laminate as a tension wave and may produce matrix cracking. The strength of the tension wave, however, in the case of sandwich panels is rather weak because the core absorbs the incoming compressive stress waves. Local transient bending waves are then initiated following several

reflections of the transient normal waves. Interlaminar stresses associated with the local bending may cause damage or if damage is present, this local bending deflection may cause the damage to propagate. Deformations due to the overall plate structural response, however, are initiated long after the transient bending and tension waves occur.

When the impact phenomenon is treated as a transient contact problem, the analysis becomes considerably more difficult. In order to simplify the analysis, past efforts by Cairns and Lagace (1989), Olsson (1992) and Lee et al. (1993) decoupled the local contact effects from the global dynamic response of the plate. In these analyses, the effect of local contact between the indentor and the plate is invoked in the global dynamic analysis through the transient response of the plate coupled with the motion of the impactor. The coupling is achieved by modelling the contact behavior between the impactor and the panel by a spring whose stiffness is obtained from experimental static indentation tests. Since the extent of the contact region and it's force distribution are not known a priori, the contact behavior between the impactor and the panel is approximated by performing static indentation tests with spherical and cylindrical indentors. This assumption facilitated the use of static indentation laws for predicting the force deformation relationship produced by the impactor. The experimental investigation of the contact behavior, however, provides only the force-indentation relation, not the extent of the contact region and the force distribution.

For damage tolerant design, accurate assessment of the stress and displacement fields is required for failure prediction of such components under transient surface loading. The presence of transverse shear deformation and the general material orthotropy coupled with transient surface loading, however, renders the analysis rather complex. In order to make the

mathematical statement of the problem tractable, several approximate solution methods were introduced. The Classical Laminate Theory (CLT) that accounts for the coupling effects of non-symmetric laminates is examined by Pister and Dong (1959), Reissner and Stavsky (1961) and Dong et al. (1962). This approach cannot account for the through-the-thickness effects because it disregards the transverse normal and shear stresses. In addition, the validity of this approach is questionable when the material properties differ appreciably from layer to layer and/or when a high degree of anisotropy exists in one or more layers as discussed by Ambartsumyan (1962). Also, the uniform displacement assumption through the thickness of a cross section becomes invalid for panels subjected to concentrated dynamic loads on the surface. Therefore, CLT is not suitable for predicting interlaminar damage caused by impact. Although it suffers from these shortcomings, it provides reasonably accurate transverse deflections for thick laminates.

In order to improve the preceding approach, Chattopadhyay (1977), Whitney and Sun (1977), Dobyns (1981), Ramkumar and Chen (1983) and Lee et al (1993) utilized Mindlin's plate theory (Mindlin, 1951) to include the effect of transverse shear deformation. Although Mindlin's plate theory is a significant improvement over the CLT, it still suffers from the inability to determine the transverse normal stress. In addition, first order shear deformation theory requires the transverse shear stiffness to be determined. The accuracy of the transverse shear stiffness depends upon a correction factor whose accurate determination is not easily achieved. An in depth discussion on the determination of this parameter is found in Noor and Burton (1990). As with the CLT, this approach also assumes uniform displacement across the thickness, and it is suitable only for moderately thick laminates. For sandwich panels, the

assumption of uniform transverse displacement is not valid because the core experiences local deformation near the impact region.

Although these investigations may provide adequately accurate results for thin plates under quasi-static loading, i.e., the time required to increase the magnitude of the applied load is longer than the period of the lowest vibration mode, their accuracy suffers if the loading rate is high, i.e. the time required to increase the magnitude of the applied load from zero to its maximum value is less than half of the natural period of the structure. Major shortcomings of these analyses arise from their inability to include the transverse normal stress which is a primary cause of delamination.

Finite element analyses employing plate and shell elements based on the aforementioned plate theories also fail to predict the transient transverse normal stress in the panel. With three-dimensional solid elements, Lee et al. (1984) and Wu and Springer (1988) modeled the laminate with several layers of elements per ply to capture the through-the-thickness effects. This type of analysis becomes computationally very intensive, however, when modelling many layers.

Consequently, a rigorous three-dimensional elasticity analysis is required to accurately determine the transient stress and displacement fields of a composite panel subjected to transverse impact. Recently, Mal and Lih (1992, 1995) utilized the exact theory of elasticity towards modeling the transient response of a unidirectional laminate subjected to concentrated and distributed surface loads. They constructed the solution for an infinite laminate by applying integral transformation techniques. Although a three-dimensional exact solution of a finite geometry laminate with arbitrary stacking sequence subjected to a static

transverse load was developed by Pagano (1970), the laminate response under transient loading does not exist. Even in the case of static analysis, the solution becomes cumbersome with different general solutions for specific laminate stacking sequences. No previous study developed an analytical method to determine the stress and displacement fields in a laminate of arbitrary stacking sequence due to a general transient surface loading.

Based on the forgoing discussion, an analytical model based on the exact theory of elasticity which is capable of dealing with contact problems is desired to accurately describe the damage induced by impact. This study provides the first part of this goal, a straightforward method to determine the transient solution of a multi-layer and finite geometry panel under transverse loading. Each of the individual layers of the panel is modeled as an elastic, homogeneous and specially orthotropic material. The finite geometry panel is supported by rollers and is subjected to an arbitrarily distributed surface load. The governing equations derived from Reissner's functional (Reissner, 1950) are solved by applying the Fourier or Laplace transformation in time while enforcing the continuity of traction and displacement components between the adjacent layers. In order to predict damage due to an impact, this analysis provides a three-dimensional exact solution for the stress and displacement fields under specified surface loading resulting from the impact event.

2. PROBLEM STATEMENT

This analysis addresses the stress and displacement fields in a composite panel subjected to transient surface loading. The geometry and loading of the panel is illustrated in Figure 1. A Cartesian reference coordinate system (x,y,z) is located at the corner on the upper surface of the panel. The length and width of the rectangular panel are denoted by "a" and "b", and it's thickness as "h". The position of the interfaces, shown in figure 2, in reference to the upper surface of the panel are specified by z^k. The thickness of the k^{th} layer is given by $t^k=z^k - z^{k-1}$.

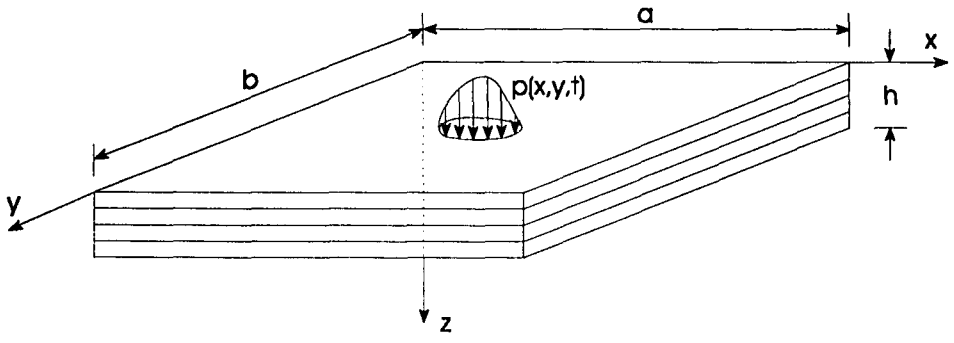

Figure 1. Panel geometry and loading configuration.

The panel is composed of layers made of homogeneous, elastic and specially orthotropic materials. Each layer has elastic moduli E_L and E_T, shear modulus G_{LT}, and Poisson's ratios ν_{TL} and ν_{TT}, where subscripts L and T are the longitudinal and transverse directions relative to the fibers. When the material and reference coordinate systems coincide, the constitutive relationship for the k^{th} layer is represented by

$$\begin{Bmatrix} \epsilon_{xx} \\ \epsilon_{yy} \\ \epsilon_{zz} \\ \epsilon_{yz} \\ \epsilon_{zx} \\ \epsilon_{xy} \end{Bmatrix}^k = \begin{bmatrix} D_{11} & D_{12} & D_{13} & 0 & 0 & 0 \\ D_{12} & D_{22} & D_{23} & 0 & 0 & 0 \\ D_{13} & D_{23} & D_{33} & 0 & 0 & 0 \\ 0 & 0 & 0 & D_{44} & 0 & 0 \\ 0 & 0 & 0 & 0 & D_{55} & 0 \\ 0 & 0 & 0 & 0 & 0 & D_{66} \end{bmatrix}^k \begin{Bmatrix} \sigma_{xx} \\ \sigma_{yy} \\ \sigma_{zz} \\ \sigma_{yz} \\ \sigma_{zx} \\ \sigma_{xy} \end{Bmatrix}^k \quad \textbf{(1)}$$

where σ_{ij} and ϵ_{ij} are the components of the stress and strain tensors, respectively and D_{ij} represents the compliance matrix with five independent constants. For balanced laminates where the material and reference coordinate systems do not coincide, a method presented in Appendix A provides an average compliance matrix. This average compliance matrix will contain the 9 independent coefficients of a specially orthotropic material.

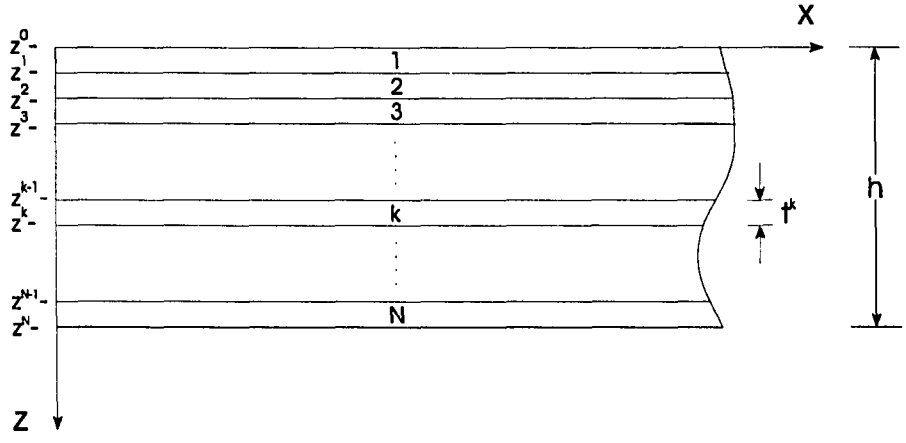

Figure 2. Identification of the layers and their position in relation to the reference frame.

As introduced by Mal et al. (1992), the dissipation of energy (material damping) in composite panels is invoked into the analysis by allowing a small percentage of the

compliance matrix to be complex. In general, the material damping is a function of the frequency, however, in this analysis the complex compliance is assumed to be a constant value for all frequencies.

The boundary conditions along the edges of the panel are representative of roller supports. The edges are free to move in the x-direction and y-direction at x=0 and x=a, and y=0 and y=b, respectively. The boundary conditions are expressed as

$$\begin{aligned} v^k = w^k = 0, \quad \sigma_{xx}^k = 0 \qquad & for x=0,\ x=a,\ 0 \le y \le b \\ u^k = w^k = 0, \quad \sigma_{yy}^k = 0 \qquad & for y=0,\ y=b,\ 0 \le x \le a \end{aligned} \tag{2}$$

where u, v and w represent the displacement components in the x, y and z directions, respectively.

The layers in the panel are treated as perfectly bonded with continuous tractions and displacements across the layer interfaces. Continuous tractions are represented as

$$\sigma_{\alpha z}^k|_{z=z^k} - \sigma_{\alpha z}^{k+1}|_{z=z^k} = 0 \qquad \alpha = x,y,z \tag{3}$$

and displacements as

$$\begin{aligned} u^k|_{z=z^k} - u^{k+1}|_{z=z^k} = 0 \\ v^k|_{z=z^k} - v^{k+1}|_{z=z^k} = 0 \\ w^k|_{z=z^k} - w^{k+1}|_{z=z^k} = 0 \end{aligned} \tag{4}$$

The $z=z^0$ surface of the panel is subjected to an arbitrary distributed load and the $z=z^N$ surface is free of tractions. The surface tractions are enforced as

$$\begin{aligned} \sigma_{\alpha z}^N|_{z=z^N} = 0 \qquad & \alpha=,x,y,z \\ \sigma_{\alpha z}^1|_{z=z^0} = 0 \qquad & \alpha=,x,y \\ \sigma_{zz}^1|_{z=z^0} = p(x,y,t) & \end{aligned} \tag{5}$$

where p(x,y,t) represents the external loading.

3. SOLUTION METHOD

In this study, the governing equations are derived by applying variational principles to Reissner's functional (Reissner, 1950), Π_R given in the form

$$\Pi_R = \int_V (\sigma^T \epsilon - \frac{1}{2}\sigma^T D \sigma - B^T u) dV - \int_{S_1} T^T u \, dS \tag{6}$$

in which $\boldsymbol{B}$, $\boldsymbol{T}$ and $\boldsymbol{u}$ are the vectors of body force, traction and displacement components and S_1 is the surface of the body over which the tractions are applied. The boldface variables represent vector or matrix quantities. In expressing the strain energy and potential energy of the applied loads, Reissner's functional treats both the stress and displacement components as dependent variables. For a transient analysis, the components of the body force vector $\boldsymbol{B}$ represent the inertial force as

$$B_x = -\rho \frac{\partial^2 u}{\partial t^2} \qquad B_y = -\rho \frac{\partial^2 v}{\partial t^2} \qquad B_z = -\rho \frac{\partial^2 w}{\partial t^2} \tag{7}$$

where ρ is the density.

Variation of the stress and displacement components over the volume of a body yields the governing Euler-Lagrange equations. For the k^{th} specially orthotropic layer of the panel, the equations become

$$D_{11}^k \sigma_{xx}^k + D_{12}^k \sigma_{yy}^k + D_{13}^k \sigma_{zz}^k - \frac{\partial u^k}{\partial x} = 0 \tag{8}$$

$$D_{12}^k \sigma_{xx}^k + D_{22}^k \sigma_{yy}^k + D_{23}^k \sigma_{zz}^k - \frac{\partial v^k}{\partial y} = 0 \tag{9}$$

$$D_{13}^k \sigma_{xx}^k + D_{23}^k \sigma_{yy}^k + D_{33}^k \sigma_{zz}^k - \frac{\partial w^k}{\partial z} = 0 \tag{10}$$

$$D_{44}^{k}\sigma_{yz}^{k} - \frac{\partial v^{k}}{\partial z} - \frac{\partial w^{k}}{\partial y} = 0 \tag{11}$$

$$D_{55}^{k}\sigma_{zx}^{k} - \frac{\partial u^{k}}{\partial z} - \frac{\partial w^{k}}{\partial x} = 0 \tag{12}$$

$$D_{66}^{k}\sigma_{xy}^{k} - \frac{\partial u^{k}}{\partial y} - \frac{\partial v^{k}}{\partial x} = 0 \tag{13}$$

$$\frac{\partial \sigma_{xx}^{k}}{\partial x} + \frac{\partial \sigma_{xy}^{k}}{\partial y} + \frac{\partial \sigma_{zx}^{k}}{\partial z} - \rho^{k}\frac{\partial^{2} u^{k}}{\partial t^{2}} = 0 \tag{14}$$

$$\frac{\partial \sigma_{xy}^{k}}{\partial x} + \frac{\partial \sigma_{yy}^{k}}{\partial y} + \frac{\partial \sigma_{yz}^{k}}{\partial z} - \rho^{k}\frac{\partial^{2} v^{k}}{\partial t^{2}} = 0 \tag{15}$$

$$\frac{\partial \sigma_{zx}^{k}}{\partial x} + \frac{\partial \sigma_{yz}^{k}}{\partial y} + \frac{\partial \sigma_{zz}^{k}}{\partial z} - \rho^{k}\frac{\partial^{2} w^{k}}{\partial t^{2}} = 0 \tag{16}$$

The time dependency in these equations is eliminated by applying either Fourier transformation

$$\hat{f}(\omega) = \int_{-\infty}^{\infty} f(t)e^{i\omega t}dt \tag{17}$$

or Laplace transformation

$$\hat{f}(s) = \int_{0}^{\infty} f(t)e^{-st}dt \tag{18}$$

where ω and s are the transformation variables. In the case of Fourier transformation, the integrand is required to vanish as time approaches infinity. Material damping introduced in the form of a complex compliance,

$$\bar{D} = D + i\epsilon D \tag{19}$$

with a small parameter, ϵ, ensures this requirement. The compliance can be treated as real

or complex for Laplace transformation as the integrand in Equation (18) converges with time. The transformed governing equations with the complex compliance become

$$\bar{D}_{11}^{k}\hat{\sigma}_{xx}^{k} + \bar{D}_{12}^{k}\hat{\sigma}_{yy}^{k} + \bar{D}_{13}^{k}\hat{\sigma}_{zz}^{k} - \frac{\partial \hat{u}^{k}}{\partial x} = 0 \tag{20}$$

$$\bar{D}_{12}^{k}\hat{\sigma}_{xx}^{k} + \bar{D}_{22}^{k}\hat{\sigma}_{yy}^{k} + \bar{D}_{23}^{k}\hat{\sigma}_{zz}^{k} - \frac{\partial \hat{v}^{k}}{\partial y} = 0 \tag{21}$$

$$\bar{D}_{13}^{k}\hat{\sigma}_{xx}^{k} + \bar{D}_{23}^{k}\hat{\sigma}_{yy}^{k} + \bar{D}_{33}^{k}\hat{\sigma}_{zz}^{k} - \frac{\partial \hat{w}^{k}}{\partial z} = 0 \tag{22}$$

$$\bar{D}_{44}^{k}\hat{\sigma}_{yz}^{k} - \frac{\partial \hat{v}^{k}}{\partial z} - \frac{\partial \hat{w}^{k}}{\partial y} = 0 \tag{23}$$

$$\bar{D}_{55}^{k}\hat{\sigma}_{zx}^{k} - \frac{\partial \hat{u}^{k}}{\partial z} - \frac{\partial \hat{w}^{k}}{\partial x} = 0 \tag{24}$$

$$\bar{D}_{66}^{k}\hat{\sigma}_{xy}^{k} - \frac{\partial \hat{u}^{k}}{\partial y} - \frac{\partial \hat{v}^{k}}{\partial x} = 0 \tag{25}$$

$$\frac{\partial \hat{\sigma}_{xx}^{k}}{\partial x} + \frac{\partial \hat{\sigma}_{xy}^{k}}{\partial y} + \frac{\partial \hat{\sigma}_{zx}^{k}}{\partial z} + \gamma^{2}\rho^{k}\hat{u}^{k} = 0 \tag{26}$$

$$\frac{\partial \hat{\sigma}_{xy}^{k}}{\partial x} + \frac{\partial \hat{\sigma}_{yy}^{k}}{\partial y} + \frac{\partial \hat{\sigma}_{yz}^{k}}{\partial z} + \gamma^{2}\rho^{k}\hat{v}^{k} = 0 \tag{27}$$

$$\frac{\partial \hat{\sigma}_{zx}^{k}}{\partial x} + \frac{\partial \hat{\sigma}_{yz}^{k}}{\partial y} + \frac{\partial \hat{\sigma}_{yz}^{k}}{\partial z} + \gamma^{2}\rho^{k}\hat{w}^{k} = 0 \tag{28}$$

in which the symbol " ^ " denotes the transformed variables and the transformation variable γ is defined as

$$\gamma^{2} = \omega^{2} = -s^{2} \tag{29}$$

To eliminate the x and y dependence, the stress and displacement components for the k^{th} layer are represented in terms of Fourier series as

$$\hat{\sigma}^k_{xx}(x,y,z,\gamma) = \sum_{m=1}^{\infty}\sum_{n=1}^{\infty} \hat{\sigma}^k_{xxmn}(z,\gamma)\sin\alpha_m x \sin\beta_n y$$

$$\hat{\sigma}^k_{yy}(x,y,z,\gamma) = \sum_{m=1}^{\infty}\sum_{n=1}^{\infty} \hat{\sigma}^k_{yymn}(z,\gamma)\sin\alpha_m x \sin\beta_n y$$

$$\hat{\sigma}^k_{zz}(x,y,z,\gamma) = \sum_{m=1}^{\infty}\sum_{n=1}^{\infty} \hat{\sigma}^k_{zzmn}(z,\gamma)\sin\alpha_m x \sin\beta_n y$$

$$\hat{\sigma}^k_{yz}(x,y,z,\gamma) = \sum_{m=1}^{\infty}\sum_{n=1}^{\infty} \hat{\sigma}^k_{yzmn}(z,\gamma)\sin\alpha_m x \cos\beta_n y$$

$$\hat{\sigma}^k_{xz}(x,y,z,\gamma) = \sum_{m=1}^{\infty}\sum_{n=1}^{\infty} \hat{\sigma}^k_{xzmn}(z,\gamma)\cos\alpha_m x \sin\beta_n y \qquad (30)$$

$$\hat{\sigma}^k_{xy}(x,y,z,\gamma) = \sum_{m=1}^{\infty}\sum_{n=1}^{\infty} \hat{\sigma}^k_{xymn}(z,\gamma)\cos\alpha_m x \cos\beta_n y$$

$$\hat{u}^k(x,y,z,\gamma) = \sum_{m=1}^{\infty}\sum_{n=1}^{\infty} \hat{u}^k_{mn}(z,\gamma)\cos\alpha_m x \sin\beta_n y$$

$$\hat{v}^k(x,y,z,\gamma) = \sum_{m=1}^{\infty}\sum_{n=1}^{\infty} \hat{v}^k_{mn}(z,\gamma)\sin\alpha_m x \cos\beta_n y$$

$$\hat{w}^k(x,y,z,\gamma) = \sum_{m=1}^{\infty}\sum_{n=1}^{\infty} \hat{w}^k_{mn}(z,\gamma)\sin\alpha_m x \sin\beta_n y$$

in which $\hat{\sigma}_{xxmn}, \hat{\sigma}_{yymn}, \ldots, \hat{w}_{mn}$ are the unknown auxiliary functions for each m and n and where $\alpha_m = m\pi/a$ and $\beta_n = n\pi/b$. Substituting the stress and displacement components in terms of their Fourier series in the governing equations leads to

$$\sum_{m=1}^{\infty}\sum_{n=1}^{\infty}\left[\bar{D}^k_{11}\hat{\sigma}^k_{xxmn} + \bar{D}^k_{12}\hat{\sigma}^k_{yymn} + \bar{D}^k_{13}\hat{\sigma}^k_{zzmn} + \hat{u}^k_{mn}\alpha_m\right]\sin\alpha_m x \sin\beta_n y = 0 \qquad (31)$$

$$\sum_{m=1}^{\infty}\sum_{n=1}^{\infty}\left[\bar{D}^k_{12}\hat{\sigma}^k_{xxmn} + \bar{D}^k_{22}\hat{\sigma}^k_{yymn} + \bar{D}^k_{23}\hat{\sigma}^k_{zzmn} + \hat{v}^k_{mn}\beta_n\right]\sin\alpha_m x \sin\beta_n y = 0 \qquad (32)$$

$$\sum_{m=1}^{\infty}\sum_{n=1}^{\infty}\left[\bar{D}^k_{13}\hat{\sigma}^k_{xxmn} + \bar{D}^k_{23}\hat{\sigma}^k_{yymn} + \bar{D}^k_{33}\hat{\sigma}^k_{zzmn} + \frac{\partial\hat{w}^k_{mn}}{\partial z}\right]\sin\alpha_m x \sin\beta_n y = 0 \qquad (33)$$

$$\sum_{m=1}^{\infty}\sum_{n=1}^{\infty}\left[\bar{D}^k_{44}\hat{\sigma}^k_{yzmn} - \frac{\partial\hat{v}^k_{mn}}{\partial z} - \hat{w}^k_{mn}\beta_m\right]\sin\alpha_m x \cos\beta_n y = 0 \qquad (34)$$

$$\sum_{m=1}^{\infty}\sum_{n=1}^{\infty}\left[\bar{D}_{55}^{k}\hat{\sigma}_{zxmn}^{k}-\frac{\partial\hat{u}_{mn}^{k}}{\partial z}-\hat{w}_{mn}^{k}\alpha_{m}\right]\cos\alpha_{m}x\,\sin\beta_{n}y=0 \tag{35}$$

$$\sum_{m=1}^{\infty}\sum_{n=1}^{\infty}\left[\bar{D}_{66}^{k}\hat{\sigma}_{xymn}^{k}-\hat{u}_{mn}^{k}\beta_{n}-\hat{w}_{mn}^{k}\alpha_{m}\right]\cos\alpha_{m}x\,\cos\beta_{n}y=0 \tag{36}$$

$$\sum_{m=1}^{\infty}\sum_{n=1}^{\infty}\left[\rho^{k}\gamma^{2}\hat{u}_{mn}^{k}+\hat{\sigma}_{xxmn}^{k}\alpha_{m}-\hat{\sigma}_{xymn}^{k}\beta_{n}+\frac{\partial\hat{\sigma}_{zxmn}^{k}}{\partial z}\right]\cos\alpha_{m}x\,\sin\beta_{n}y=0 \tag{37}$$

$$\sum_{m=1}^{\infty}\sum_{n=1}^{\infty}\left[\rho^{k}\gamma^{2}\hat{v}_{mn}^{k}-\hat{\sigma}_{xymn}^{k}\alpha_{m}+\hat{\sigma}_{yymn}^{k}\beta_{n}+\frac{\partial\hat{\sigma}_{yzmn}^{k}}{\partial z}\right]\sin\alpha_{m}x\,\cos\beta_{n}y=0 \tag{38}$$

$$\sum_{m=1}^{\infty}\sum_{n=1}^{\infty}\left[\rho^{k}\gamma^{2}\hat{w}_{mn}^{k}-\hat{\sigma}_{zxmn}^{k}\alpha_{m}-\hat{\sigma}_{yzmn}^{k}\beta_{n}+\frac{\partial\hat{\sigma}_{zzmn}^{k}}{\partial z}\right]\sin\alpha_{m}x\,\sin\beta_{n}y=0 \tag{39}$$

The Fourier series representation of the loading function in terms of the transformation variable becomes

$$\hat{p}(x,y,\gamma)=\sum_{m=1}^{\infty}\sum_{n=1}^{\infty}\hat{p}_{mn}(\gamma)\sin\alpha_{m}x\,\sin\beta_{n}y \tag{40}$$

with the Fourier series coefficient expressed as

$$\hat{p}_{mn}(\gamma)=\frac{4}{ab}\int_{a}^{b}\int_{a}^{b}\hat{p}(x,y,\gamma)\,\sin\alpha_{m}x\,\sin\beta_{n}y\,dxdy \tag{41}$$

For arbitrary x and y in Equations (31) through (39), the resulting ordinary differential equations corresponding to specific m and n can be expressed in matrix form as

$$\begin{bmatrix}M_{11} & M_{12}\\ M_{21} & M_{22}\end{bmatrix}^{k}\begin{Bmatrix}F\\ S\end{Bmatrix}^{k}+\begin{bmatrix}0 & 0\\ 0 & N_{22}\end{bmatrix}^{k}\begin{Bmatrix}\frac{\partial F}{\partial z}\\ \frac{\partial S}{\partial z}\end{Bmatrix}^{k}=\begin{Bmatrix}0\\ 0\end{Bmatrix} \tag{42}$$

where

$$F^k = \begin{Bmatrix} \hat{\sigma}_{xxmn} \\ \hat{\sigma}_{yymn} \\ \hat{\sigma}_{xymn} \end{Bmatrix}^k \quad , \quad S^k = \begin{Bmatrix} \hat{\sigma}_{yzmn} \\ \hat{\sigma}_{zzmn} \\ \hat{\sigma}_{zzmn} \\ \hat{u}_{mn} \\ \hat{v}_{mn} \\ \hat{w}_{mn} \end{Bmatrix}^k \tag{43}$$

$$M_{11}{}^k = \begin{bmatrix} \bar{D}_{11} & \bar{D}_{12} & 0 \\ \bar{D}_{12} & \bar{D}_{22} & 0 \\ 0 & 0 & \bar{D}_{66} \end{bmatrix}^k \quad , \quad M_{12}{}^k = M_{21}{}^{kT} = \begin{bmatrix} 0 & 0 & \bar{D}_{13} & \alpha_m & 0 & 0 \\ 0 & 0 & \bar{D}_{23} & 0 & \beta_n & 0 \\ 0 & 0 & 0 & -\beta_n & -\alpha_m & 0 \end{bmatrix}^k \tag{44}$$

and

$$M_{22}{}^k = \begin{bmatrix} \bar{D}_{44} & 0 & 0 & 0 & 0 & -\beta_n \\ 0 & \bar{D}_{55} & 0 & 0 & 0 & -\alpha_m \\ 0 & 0 & \bar{D}_{33} & 0 & 0 & 0 \\ 0 & 0 & 0 & \gamma^2\rho & 0 & 0 \\ 0 & 0 & 0 & 0 & \gamma^2\rho & 0 \\ -\beta_n & -\alpha_m & 0 & 0 & 0 & \gamma^2\rho \end{bmatrix} \tag{45}$$

The matrix representation of the governing differential equations permits the expression of the vector F^k containing the in-plane stress coefficients in terms of the vector S^k containing the displacement and out-of -plane stress coefficients as

$$F^k = - M_{11}^{k^{-1}} M_{12}^k S^k \tag{46}$$

Substituting for F^k in Equation (42) results in the coupled system of first order ordinary differential equations

$$\frac{\partial S^k}{\partial z} + K^k S^k = 0 \tag{47}$$

with

$$\boldsymbol{K}^{k} = \boldsymbol{N}_{22}^{k-1}\left[-\boldsymbol{M}_{12}^{k\,T}\,\boldsymbol{M}_{11}^{k-1}\,\boldsymbol{M}_{12}^{k} + \boldsymbol{M}_{22}^{k}\right] \tag{48}$$

The solution to the homogeneous system of equations is readily constructed by assuming

$$\boldsymbol{S}^{k} = \boldsymbol{C}^{k} e^{-\lambda^{k} z} \tag{49}$$

In constructing the solution, the determinant of the system of equations is required to vanish for a non-trivial solution to exist. The characteristic equation for the k^{th} layer takes the form

$$(\lambda^{k})^{6} + L^{k}(\lambda^{k})^{4} + M^{k}(\lambda^{k})^{2} + N^{k} = 0 \tag{50}$$

with L^k, M^k and N^k expressed in terms of the components of $\boldsymbol{K}^k$. This form of the characteristic equation reveals that three of the roots (eigenvalues) are the opposite sign of the remaining ones as λ^k_1, λ^k_2, λ^k_3, $-\lambda^k_1$, $-\lambda^k_2$, and $-\lambda^k_3$. The coupled system of equations can be decoupled by allowing

$$\boldsymbol{S}^{k} = \boldsymbol{Q}^{k}\boldsymbol{R}^{k} \tag{51}$$

where $\boldsymbol{Q}^k$ is the transformation matrix of eigenvectors.

The decoupled system of equations becomes

$$\frac{\partial \boldsymbol{R}^{k}}{\partial z} + \boldsymbol{\Lambda}^{k}\boldsymbol{R}^{k} = 0 \tag{52}$$

in which $\boldsymbol{\Lambda}^k$ is a diagonal matrix composed of the eigenvalues. By the procedure developed by Mal (1988), the solution to the decoupled system of equations is written as

$$R^k(z) = E^k(z)C^k = \begin{bmatrix} e^{-\lambda_1 z} & 0 & 0 & 0 & 0 & 0 \\ 0 & e^{-\lambda_2 z} & 0 & 0 & 0 & 0 \\ 0 & 0 & e^{-\lambda_3 z} & 0 & 0 & 0 \\ 0 & 0 & 0 & e^{\lambda_1 z} & 0 & 0 \\ 0 & 0 & 0 & 0 & e^{\lambda_2 z} & 0 \\ 0 & 0 & 0 & 0 & 0 & e^{\lambda_3 z} \end{bmatrix}^k \begin{Bmatrix} C_1 \\ C_2 \\ C_3 \\ C_4 \\ C_5 \\ C_6 \end{Bmatrix}^k \tag{53}$$

Using the transformation matrix, Q^k, the solution for the out-of-plane stress and displacement coefficients becomes

$$S^k(z) = Q^k E^k(z) C^k \tag{54}$$

Prior to enforcing the boundary and continuity conditions so as to determine the constants C^k for each layer, the E^k matrix is multiplied by a vector of constants (the first and second three rows by $e^{\lambda_i z^k}$ and $e^{-\lambda_i z^{k-1}}$, respectively) so that it takes the form

$$E^k(z) = \begin{bmatrix} e^{\lambda_1^k(z^k - z)} & 0 & 0 & 0 & 0 & 0 \\ 0 & e^{\lambda_2^k(z^k - z)} & 0 & 0 & 0 & 0 \\ 0 & 0 & e^{\lambda_3^k(z^k - z)} & 0 & 0 & 0 \\ 0 & 0 & 0 & e^{\lambda_1^k(z - z^{k-1})} & 0 & 0 \\ 0 & 0 & 0 & 0 & e^{\lambda_2^k(z - z^{k-1})} & 0 \\ 0 & 0 & 0 & 0 & 0 & e^{\lambda_3^k(z - z^{k-1})} \end{bmatrix} \tag{55}$$

In the case of the k^{th} layer, the matrix E^k is evaluated at the k-1 interface as

$$E^k(z^{k-1}) = \begin{bmatrix} E_t & 0 \\ 0 & I \end{bmatrix}^k \tag{56}$$

where I is a 3x3 identity matrix and

$$E_t^k = \begin{bmatrix} e^{\lambda_1 t} & 0 & 0 \\ 0 & e^{\lambda_2 t} & 0 \\ 0 & 0 & e^{\lambda_3 t} \end{bmatrix}^k \tag{57}$$

with t^k equal to the thickness of the k^{th} layer. Similarly, for the k^{th} interface of the k^{th} layer,

$$E^k(z^k) = \begin{bmatrix} I & 0 \\ 0 & E_t \end{bmatrix}^k \tag{58}$$

Decomposing the vector S^k in the form

$$S^k(z) = \begin{Bmatrix} T(z) \\ U(z) \end{Bmatrix}^k \tag{59}$$

with

$$T^{kT} = \left[\hat{\sigma}_{yzmn} \quad \hat{\sigma}_{zzmn} \quad \hat{\sigma}_{szmn} \right] \tag{60}$$

and

$$U^{kT} = \left[\hat{u}_{mn} \quad \hat{v}_{mn} \quad \hat{w}_{mn} \right] \tag{61}$$

permits the equations for the stress and displacement coefficients at the k-1 and k interfaces to be rewritten as

$$\begin{Bmatrix} T(z^{k-1}) \\ U(z^{k-1}) \end{Bmatrix}^k = \begin{bmatrix} Q_{11} & Q_{12} \\ Q_{21} & Q_{22} \end{bmatrix}^k \begin{bmatrix} E_t & 0 \\ 0 & I \end{bmatrix}^k \begin{Bmatrix} C_+ \\ C_- \end{Bmatrix}^k \tag{62}$$

and

$$\begin{Bmatrix} T(z^k) \\ U(z^k) \end{Bmatrix}^k = \begin{bmatrix} Q_{11} & Q_{12} \\ Q_{21} & Q_{22} \end{bmatrix}^k \begin{bmatrix} I & 0 \\ 0 & E_t \end{bmatrix}^k \begin{Bmatrix} C_+ \\ C_- \end{Bmatrix}^k \tag{63}$$

respectively, where Q_{ij} are the submatricies of the transformation matrix Q. The vectors C_+^k and C_-^k contain the unknown coefficients consistent with the partitioning of the matrix Q^k for

each layer.

The boundary conditions at the $z=z^0$ and $z=z^N$ surfaces can be expressed as

$$T^1(z^0) = \begin{Bmatrix} 0 \\ 0 \\ \hat{P}_{mn} \end{Bmatrix} = Q_{11}^1 E_t^1 C_+^1 + Q_{12}^1 C_-^1 \tag{64}$$

and

$$T^N(z^N) = \begin{Bmatrix} 0 \\ 0 \\ 0 \end{Bmatrix} = Q_{11}^N C_+^N + Q_{12}^N E_t^N C_-^N \tag{65}$$

respectively. A recursive relationship is then established to enforce the continuity of out-of-plane stresses and displacements between the k and k+1 interfaces as

$$Q_{11}^k C_+^k + Q_{12}^k E_t^k C_-^k - Q_{11}^{k+1} E_t^{k+1} C_+^{k+1} - Q_{12}^{k+1} C_-^{k+1} = 0 \tag{66}$$

$$Q_{21}^k C_+^k + Q_{22}^k E_t^k C_-^k - Q_{21}^{k+1} E_t^{k+1} C_+^{k+1} - Q_{22}^{k+1} C_-^{k+1} = 0 \tag{67}$$

The boundary and continuity conditions are then rewritten in Equation (68) to form the algebraic equations to determine the unknown layer coefficients C_+^k and C_-^k.

$$\begin{bmatrix} Q_{11}^1 E_t^1 & Q_{12}^1 & 0 & 0 & & & & \\ Q_{11}^1 & Q_{12}^1 E_t^1 & -Q_{11}^2 E_t^2 & -Q_{12}^2 & & & & \\ Q_{21}^1 & Q_{22}^1 E_t^1 & -Q_{21}^2 E_t^2 & -Q_{22}^2 & & & & \\ & & \ddots & \ddots & \ddots & & & \\ & & & & Q_{11}^{N-1} & Q_{12}^{N-1} E_t^{N-1} & -Q_{11}^N E_t^N & -Q_{12}^N \\ & & & & Q_{21}^{N-1} & Q_{22}^{N-1} E_t^{N-1} & -Q_{21}^N E_t^N & -Q_{22}^N \\ & & & & 0 & 0 & Q_{11}^N & Q_{12}^N E_t^N \end{bmatrix} \begin{Bmatrix} C_+^1 \\ C_-^1 \\ C_+^2 \\ C_-^2 \\ \vdots \\ \vdots \\ C_+^{N-1} \\ C_-^{N-1} \\ C_+^N \\ C_-^N \end{Bmatrix} = \begin{Bmatrix} T^1(z^0) \\ 0 \\ 0 \\ 0 \\ \vdots \\ \vdots \\ 0 \\ 0 \\ 0 \\ 0 \end{Bmatrix} \tag{68}$$

The solution to this system of algebraic equations leads to the out-of-plane stress and

displacement coefficients through the substitution of $\boldsymbol{C}^k$ into Equation (54) where $\boldsymbol{E}^k$ takes the form of Equation (55). The in-plane stress coefficients are then obtained through Equation (46). The process of determining the stress and displacement coefficients is repeated for each value of m and n in the Fourier series summation.

The stress and displacement components determined as a function of the transformation variable are then transformed back to the time domain through Fourier inversion,

$$f(t) = \frac{1}{2\pi}\int_{-\infty}^{\infty} \hat{f}(\omega)e^{-i\omega t}dw \tag{69}$$

or Laplace inversion,

$$f(t) = \frac{1}{2\pi i}\int_{c-i\infty}^{c+i\infty} \hat{f}(s)e^{st}ds \tag{70}$$

4. NUMERICAL RESULTS

The results in the time domain are obtained by performing numerical inversions of Fourier or Laplace transformations. In order to establish the accuracy of the numerical Laplace and Fourier inversion methods, a simple ordinary differential equation is solved and their solutions are compared with the analytic solution. A quasi-static response of a laminate is considered to validate the present analysis with a known exact solution given by Pagano (1970). After validating the present analysis, two transient analyses are performed to investigate the response of thin and thick laminates. The solution concerning the thin laminate is compared with that of a finite element analysis. Finally, the transient response of a sandwich panel with and absorptive core is examined for two damping parameters.

4.1 Fast Fourier Inversion and the Inverse Laplace Transform

In order to validate the numerical inversion process employed in this study a simple ordinary differential equation given as

$$\ddot{y} + \epsilon\dot{y} + y = \delta(t) \tag{71}$$

with the initial conditions

$$y(0) = 0, \quad \dot{y}(0) = 0 \tag{72}$$

is examined. The analytical solution to the differential equation is

$$y(t) = \frac{e^{-\frac{\epsilon}{2}+\frac{\sqrt{\epsilon^2-4}}{2}} - e^{-\frac{\epsilon}{2}-\frac{\sqrt{\epsilon^2-4}}{2}}}{\sqrt{\epsilon^2-4}} \tag{73}$$

Applying the Fourier and Laplace transformations to the differential equation gives

$$\hat{y}(\omega) = \frac{1}{1 - \epsilon\omega i - \omega^2} \tag{74}$$

and

$$\hat{y}(s) = \frac{1}{1 + \epsilon s + s^2} \tag{75}$$

respectively.

To determine the inverse Fourier transform of Equation (74), an inverse fast Fourier transform (FFT) is performed at 1024 points between 0 and 50. The Fourier transform of a function only exists if the integrand in Equation (17) converges to zero. Care must be taken when performing the numerical fast Fourier transform to ensure that the integrand in both the time and frequency domain has converged to zero within the sampling period. This is accomplished simply by performing the analysis several times, examining the results, and making the appropriate changes in the time period or number of points.

The inverse Laplace transform scheme is based upon a series summation which is performed until a specified accuracy is attained. It must be noted, however, that this routine does not converge in an acceptable time for all functions and the Fourier transformation scheme is generally more efficient. The Laplace inversion was performed at 100 points between 0 and 20. As shown in Figure 3, excellent agreement is found between the analytic solution, the fast Fourier inversion, and Laplace inversion schemes between 0 and 20.

3

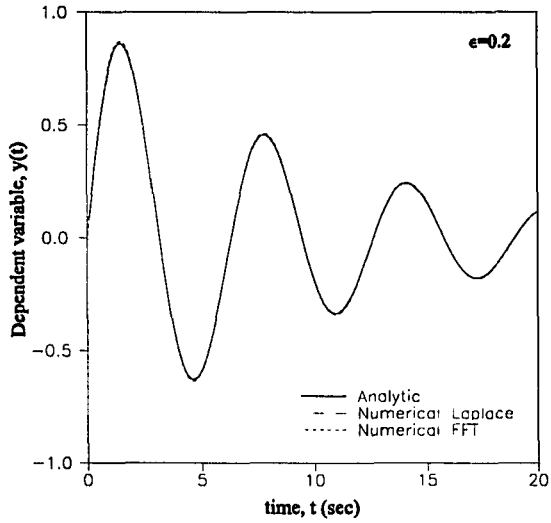

Figure 3. Verification of the numerical inversion process

4.2 Static Thick Laminate Analysis

In order to verify the present analysis, a statically loaded rectangular panel is considered and the results are compared with the well known exact solution by Pagano (1970). The static sinusoidal loading is prescribed by the function given as

$$p(x,y) = \sigma \sin\frac{\pi}{a}x \sin\frac{\pi}{b}y \qquad (76)$$

where σ is the amplitude of the loading. The plate is of length a in the x-direction and of width b=3a in the y-direction. The span to thickness ratio, s (s=a/h), is equal to 4.

Noting that Pagano's material is not transversely isotropic, the material coefficients used in the analysis are

$$
\begin{aligned}
E_L &= 25.x10^6\ psi \\
E_T &= 1.0x10^6\ psi \\
G_{LT} &= 0.5x10^6\ psi \\
G_{TT} &= 0.2x10^6\ psi \\
\nu_{LT} &= \nu_{TT} = 0.25
\end{aligned}
\tag{77}
$$

and the panel's lay-up is [0°/90°/0°].

A simple modification to the present formulation is required to determine the static solution. This is achieved by setting the body force terms in Reissner's functional equal to zero. It is identical to solving the transient analysis with the transformation variable equal to zero.

For direct comparison with the results provided by Pagano, the stress and displacement components are normalized as

$$
\begin{aligned}
\left[\sigma^*_{xx}, \sigma^*_{yy}, \sigma^*_{xy}\right] &= \frac{1}{\sigma s^2}\left[\sigma_{xx}, \sigma_{yy}, \sigma_{xy}\right] \\
\left[\sigma^*_{xz}, \sigma^*_{yz}\right] &= \frac{1}{\sigma s}\left[\sigma_{xz}, \sigma_{yz}\right] \\
w^* &= \frac{100 E_T w}{\sigma h s^4}
\end{aligned}
\tag{78}
$$

and a comparison of the results are presented Table 1. Excellent agreement is found between Pagano's solution and the present analysis. For reasons previously discussed, the solution provided by CLT is expected and does differ greatly from the solutions provided by Pagano and this analysis.

Normalized Stress and Displacement	Present analysis	Pagano (1970)	
		Exact Solution	CLT
$\sigma^*_{xx}(a/2,b/2,0)$	1.14	1.14	0.623
$\sigma^*_{xx}(a/2,b/2,h)$	-1.10	-1.10	-0.623
$\sigma^*_{yy}(a/2,b/2,h/3)$	0.108	0.109	0.0252
$\sigma^*_{zx}(0,b/2,h/2)$	0.351	0.351	0.440
$\sigma^*_{yz}(a/2,0,h/2)$	0.0327	0.0334	0.0108
$\sigma^*_{xy}(0,0,0)$	-0.0268	-0.0269	-0.0083
$\sigma^*_{xy}(0,0,h)$	0.0282	0.0281	0.0083
$w^*(a/2,b/2,h/2)$	2.82	2.82	0.503

Table 1. Normalized solutions for Pagano, CLT and the present analysis.

4.3 Transient Thin Laminate Analysis

A transient analysis is performed on a thin square laminate. The panel is 10 inches by 10 inches with a thickness of 0.25 inches. The laminate consists of 3 layers of equal thickness with a lay-up of [0°/90°/0°]. The material properties are the same as those given by Pagano and the density of the material is $2.5\text{x}10^{-4}$ slugs/in^3.

The panel is subjected to a non-uniform distributed load applied over a 2 inch by 2 inch square at the center of the plate. The loading is represented by $p(x,y,t)=g(x,y)h(t)$ where

$$g(x,y) = -(x-4)^2(x-6)^2(y-4)^2(y-6)^2 \quad ; \quad \begin{matrix} 4 \le x \le 6 \\ 4 \le y \le 6 \end{matrix} \tag{79}$$

and

$$h(t) = \begin{cases} 1 & ; \quad t \le 0.001 \text{ sec.} \\ 0 & ; \quad t > 0.001 \text{ sec.} \end{cases} \tag{80}$$

The function $g(x,y)$ is chosen for it's spatially smooth loading distribution; thus, it requires

relatively few terms to approximate the function in a Fourier series. Fifteen terms in the Fourier series representation provides an adequate approximation to the given loading function, $g(x,y)$, across the surface of the plate as shown in Figure 4.

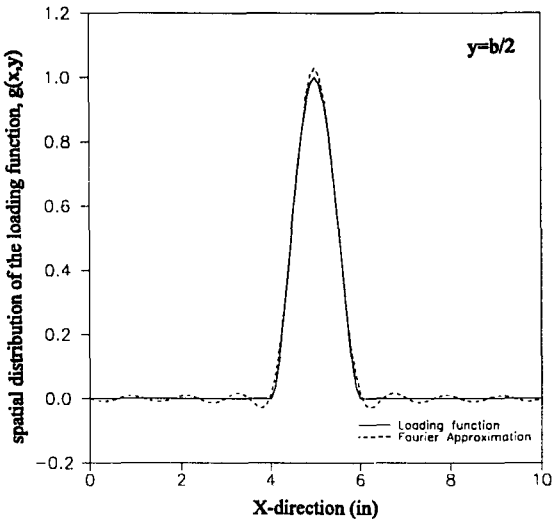

Figure 4. Comparison of the Fourier series representation and the actual loading function.

Both Fourier and Laplace transformation methods can solve the transient problem. An inverse fast Fourier transform is performed at 16384 points between 0 and 1 second. The damping parameter, ϵ, ensuring the integrand in Equation (17) to be convergent, is taken as 0.025. This small parameter provides an essentially elastic solution with minimal damping. Although the period just subsequent to the impact is of interest, the 1 second time period is required to allow the panel's vibrations to attenuate. Upon completion, only the time period up to 0.0015 seconds is examined as shown in Figures 5 through 10.

Laplace transformation is also used to determine the transient response. As stated

previously, the numerical routine which is used to determine the inverse Laplace transform does not converge efficiently for all functions. Therefore, only the displacement at a point will be examined and compared with the results obtained from the Fourier transformation and the finite element analysis. For the other stress and displacement components, the inverse FFT proves to be a more efficient method.

The results obtained by the Laplace and Fourier transformations are compared with a solution constructed by the finite element analysis (FEA) program ABAQUS (Pawtucket, RI). In the finite element analysis, the square plate is modeled with a twenty by twenty square element mesh. The elements utilized in the analysis are of ABAQUS type S8R. These elements are eight node shell elements with reduced integration. Although these shell elements are developed from the classical plate theory, they are intended to model thick panels, where estimates of the interlaminar shear stresses are required. Unlike the in-plane stresses, the transverse shear stresses are not calculated from the constitutive behavior of the shell. Instead, subsequent to the analysis, ABAQUS estimates the transverse shear stresses based on a piecewise quadratic variation of the transverse shear stress across the section, under pure bending about one axis. These elements are still, however, incapable of determining the transverse normal stress.

A comparison of the finite element results with those determined by the present analysis are presented in Figures 5 through 10. Excellent agreement is found for the transverse displacement between the three solution methods suggesting the small damping parameter included in the Fourier transformation formulation has relatively little effect shortly after the impact event. Close agreement is also observed between the ABAQUS solutions

and Fourier transformation solutions for the in-plane and transverse shear stresses.

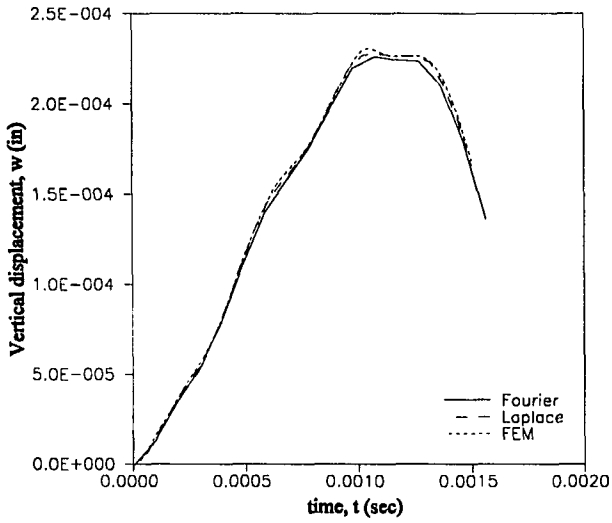

Figure 5. Variation of the vertical displacement, w as a function of time for the thin laminate at x=5.5, y=5.5, and z=h/3.

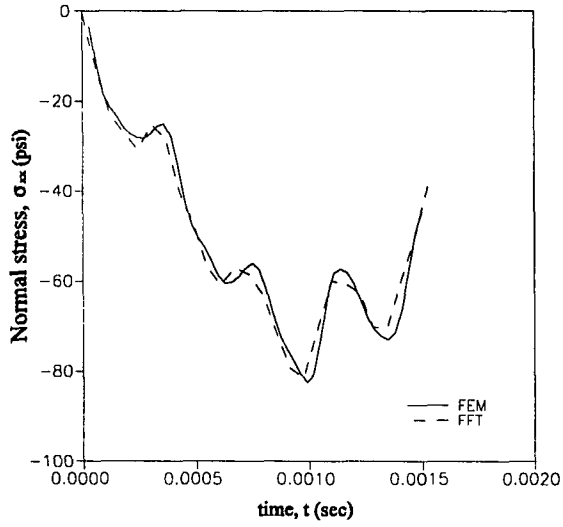

Figure 6. Variation of the normal stress, σ_{xx} as a function of time for the thin laminate at x=5.5, y=5.5, and z=0.

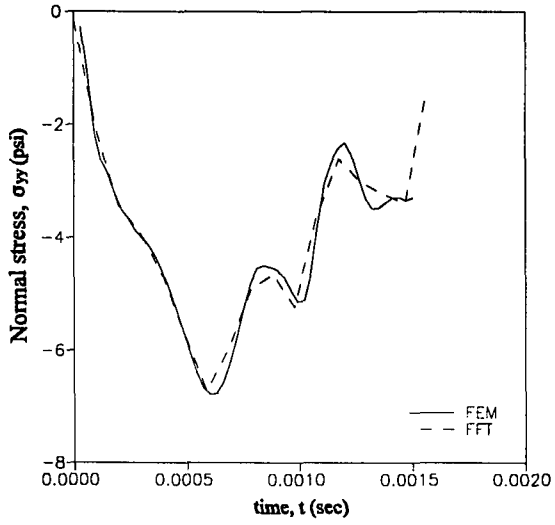

Figure 7. Variation of the normal stress, σ_{yy} as a function of time for the thin laminate at x=5.5, y=5.5, and z=0.

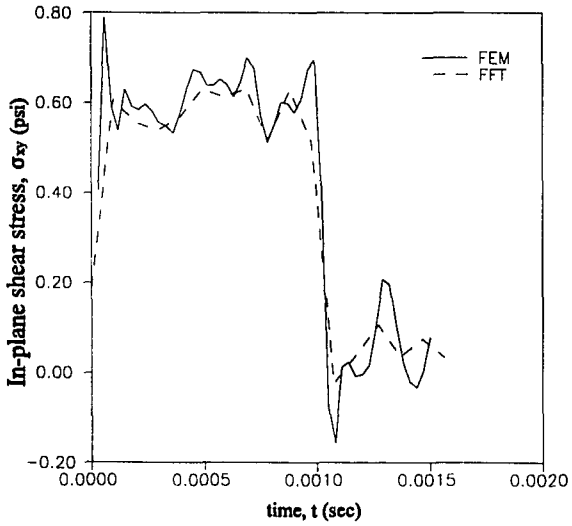

Figure 8. Variation of the in-plane shear stress, σ_{xy} as a function of time for the thin laminate at x=5.5, y=5.5, and z=0.

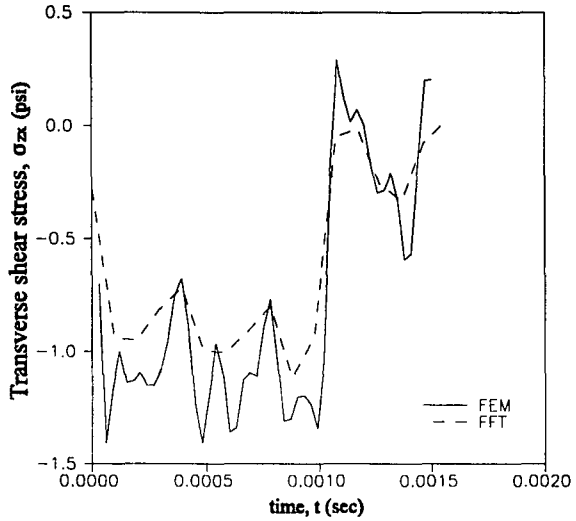

Figure 9. Variation of the transverse shear stress, σ_{zx} as a function of time for the thin laminate at x=5.5, y=5.5, and z=h/3.

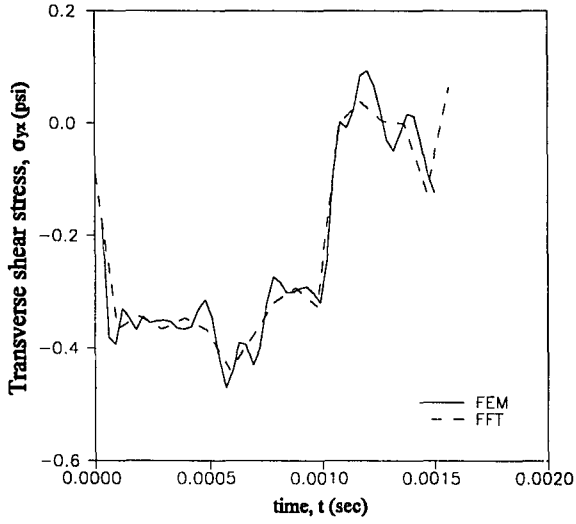

Figure 10. Variation of the transverse shear stress, σ_{yz} as a function of time for the thin laminate at x=5.5, y=5.5, and z=h/3.

4.4 Transient Thick Laminate Analysis

The next analysis is concerned with a thick square laminate with an edge length of 5 inches and the thickness of 1 inch. The panel is 3 layers of equal thickness oriented [0°/90°/0°]. The material coefficients and density are the same as in the thin plate analysis.

A loading function similar to that of the preceding analysis is used for the thick laminate; it's distribution is over a 1 inch square patch at the center of the plate. The loading function P(x,y,t)=g(x,y)h(t) is represented as

$$g(x,y) = -25600\,(x-2)^2(x-3)^2(y-2)^2(y-3)^2 \quad ; \quad \begin{matrix} 2 \le x \le 3 \\ 2 \le y \le 3 \end{matrix} \tag{81}$$

and

$$h(t) = \begin{cases} 1 & ; \quad t \le 0.001 \text{ sec.} \\ 0 & ; \quad t > 0.001 \text{ sec.} \end{cases} \tag{82}$$

The Fourier series representation of this also involves 15 terms. The Fourier inversion is performed at 16384 points between 0 and 0.75 seconds. As before, a damping parameter of 0.025 is sufficient to cause the panel's vibrations to attenuate during the time period.

The vertical displacement is compared with the solution of a finite element analysis. The finite element model is again constructed of a 20 by 20 square element mesh with the specified distributed load applied at the center of the laminate. The variation of the vertical displacement as a function of time can be observed in Figure 11. A more noticeable difference exists between the two solutions than that of the thin laminate analysis. The damping factor is not believed to be the source of the difference since the solution provided by the Fourier transform precedes the finite element analysis solution.

Normal and shear stresses as determined by the Fourier transformation analysis are

presented in Figures 12 through 16. Since the finite element analysis is based upon thin plate assumptions, the stresses are not included in the comparison.

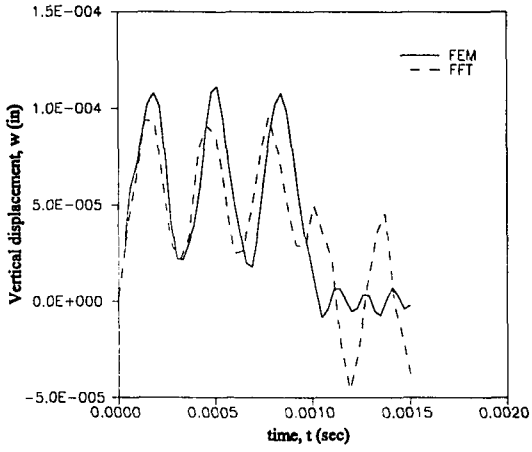

Figure 11. Variation of the vertical displacement, w as a function of time for the thick laminate at x=2.75, y=2.75 and z=h/3.

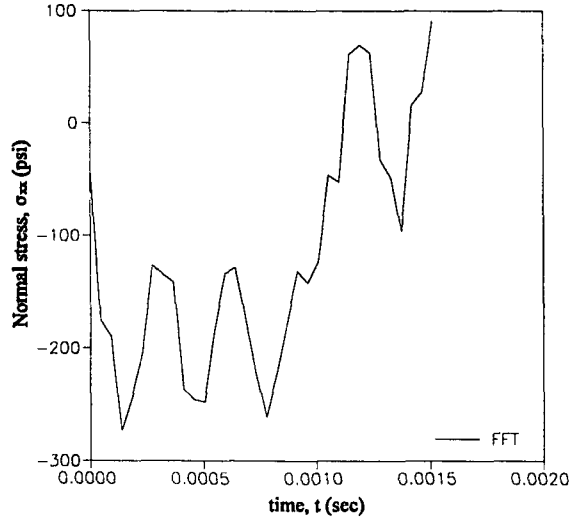

Figure 12. Variation of the normal stress, σ_{xx} as a function of time for the thick laminate at x=2.75, y=2.75 and z=0.

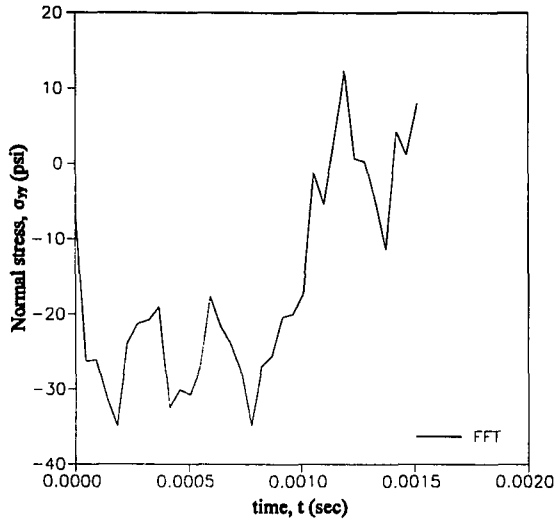

Figure 13. Variation of the normal stress, σ_{yy} as a function of time for the thick laminate at x=2.75, y=2.75 and z=0.

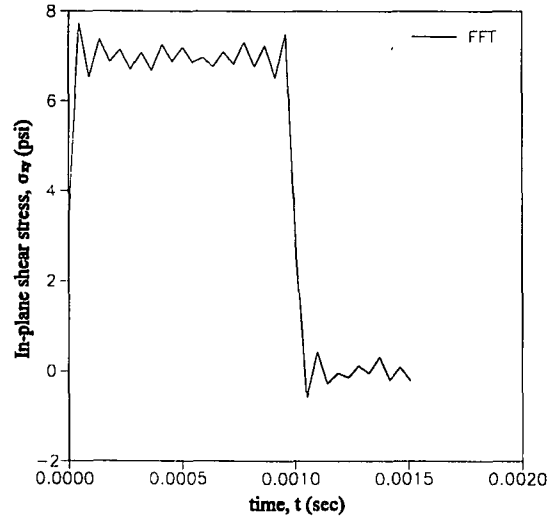

Figure 14. Variation of the in-plane shear stress, σ_{xy} as a function of time for the thick laminate at x=2.75, y=2.75 and z=0.

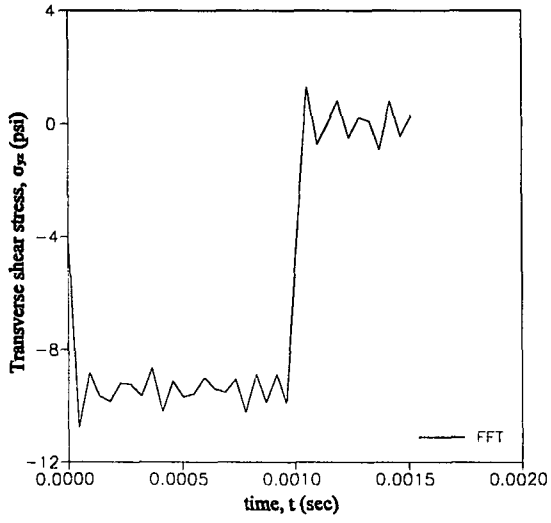

Figure 15. Variation of the transverse shear stress, σ_{yz} as a function of time for the thick laminate at x=2.75, y=2.75 and z=h/3.

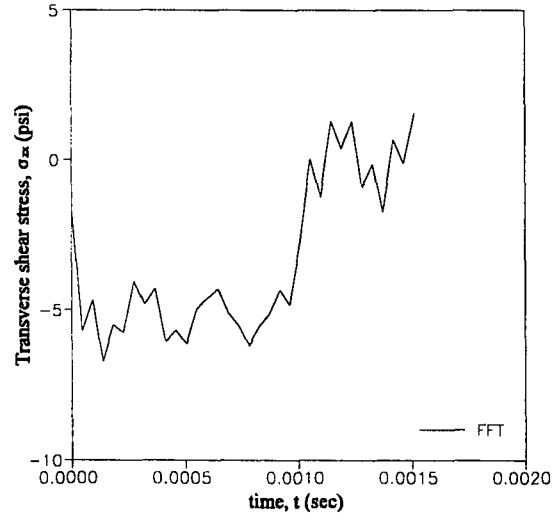

Figure 16. Variation of the transverse shear stress, σ_{zx} as a function of time for the thick laminate at x=2.75, y=2.75 and z=h/3.

4.5 Transient Sandwich Panel Analysis

A sandwich panel with elastic face sheets and an absorptive core is subjected to transverse impact. The panel is composed of layers with a stacking sequence of [0°/90°/core/90°/0°]. The material properties of the elastic face sheets are the same as those used by Pagano. The transversely isotropic material properties of the core are

$$\begin{aligned} E_{TT} &= 0.04x10^{6}\ psi \\ E_{LL} &= 0.5x10^{6}\ psi \\ G_{LT} &= 0.06x10^{6}\ psi \\ \nu_{TT} &= \nu_{TL} = 0.25 \end{aligned} \tag{83}$$

and the density of the 3 pound core is $5.4\text{x}10^{-5}$ slugs/in^3. The panel is 10 inches square and the thickness of the plies and core are 0.02 and 0.5 inches, respectively. The panel is subjected to the loading distribution, p(x,y,t)=g(x,y)h(t) where

$$g(x,y) = -100\,(x-4)^2(x-6)^2(y-4)^2(y-6)^2 \quad ; \quad \begin{matrix} 4 \le x \le 6 \\ 4 \le y \le 6 \end{matrix} \tag{84}$$

and

$$h(t) = \begin{cases} 1 & ; \quad t \le 0.001\ \text{sec.} \\ 0 & ; \quad t > 0.001\ \text{sec.} \end{cases} \tag{85}$$

Two different damping parameters, 0.025 and 0.1, are considered. A numerical inverse fast Fourier transform is applied with 16384 points over time periods of 1.0 and 0.8 seconds for the lightly and heavily damped cases, respectively. Again, the panel's vibrations attenuate within the specified time periods.

The displacement of a point located beneath the loading surface at the core/face sheet interface (x=5.5, y=5.5 and z=0.04) versus time is presented in Figure 17. The results reveal that the stress and displacement fields are highly dependent upon the amount of damping used

in the analysis. The displacement of the lightly damped panel oscillates at a higher frequency than the panel with a damping parameter of 0.1. The normal stresses σ_{xx} and σ_{yy} respond in a comparable manner with the stresses in the lightly damped panel preceding the heavily damped panel as displayed in Figures 18 and 19. The in-plane and transverse shear stresses are observed in Figures 20 through 21 to respond in a manner consistent with the overall bending of the plate.

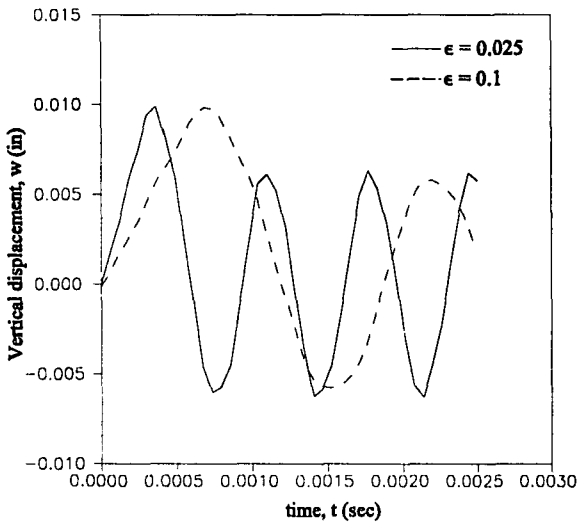

Figure 17. Variation of the vertical displacement, w as a function of time for the sandwich panel.

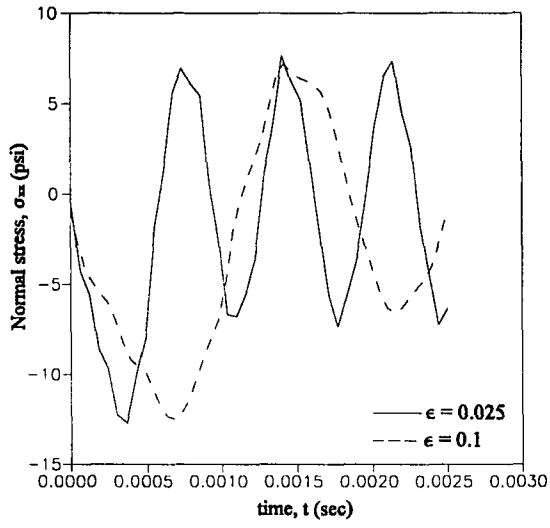

Figure 18. Variation of the normal stress, σ_{xx} as a function of time for the sandwich panel.

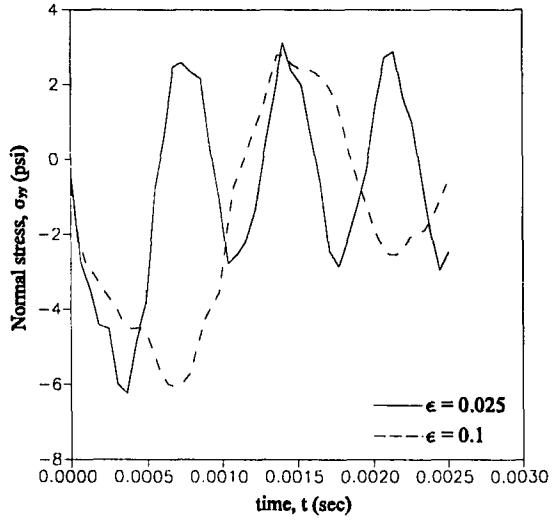

Figure 19. Variation of the normal stress, σ_{yy} as a function of time for the sandwich panel.

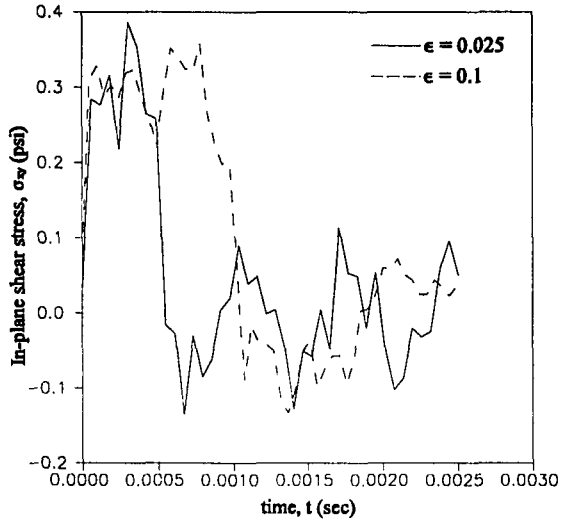

Figure 20. Variation of the in-plane shear stress, σ_{xy} as a function of time for the sandwich panel.

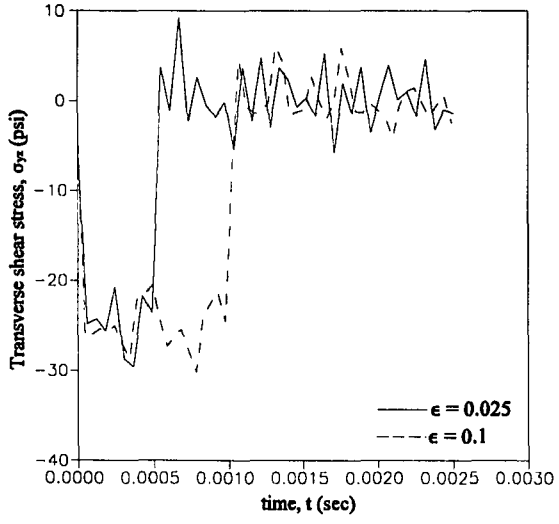

Figure 21. Variation of the transverse shear stress, σ_{yz} as a function of time for the sandwich panel.

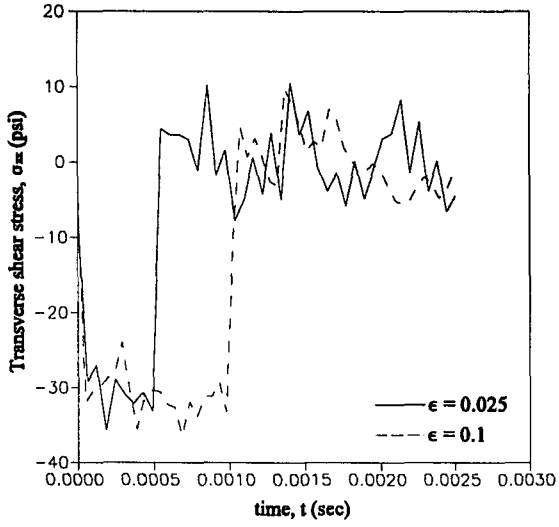

Figure 22. Variation of the transverse shear stress, σ_{zx} as a function of time for the sandwich panel.

5. DISCUSSION

In order to predict damage due to an impact, this analysis provides a three-dimensional exact solution for the stress and displacement fields under specified surface loading resulting from transverse impact. A multi-layer rectangular panel consisting of elastic, homogeneous and specially orthotropic layers is supported by rollers and is subjected to an arbitrary transverse loading distribution. The governing equations derived from Reissner's functional are solved by applying the Fourier or Laplace transformation in time while enforcing the continuity of tractions and displacements. In this manner, the exact stress and displacement fields required for damage characterization are determined.

The first verification study performed was to determine the accuracy of the numerical routines used to invert the Fourier and Laplace transformations. For the case of the ordinary differential equation, the inverse Fourier and inverse Laplace transformations provide excellent results. The numerical inversion of the Laplace transformation is based upon a series summation which, in the case of the thin panel analysis is found to be computationally very intensive for quantities such as the transverse normal and in-plane shear stresses. The numerical inversion of Fourier transformation routines proved to be rather robust and straightforward.

The present solution method was verified by comparing the static results from this analysis with those provided by Pagano (1970). The comparison yields remarkable agreement between this analysis and Pagano's solution and demonstrates the CLT's inability to accurately model relatively thick laminates.

The finite element method was used to construct the transient solution of a thin multi-

layer panel subject to a transverse loading distribution. The transverse displacement results of the inverse Fourier and inverse Laplace transformations were compared with the results of the finite element analysis and are in close agreement. The Laplace transformation scheme was not utilized to find the other stress and displacement components for the reasons discussed previously. Because the plate elements used in the finite element analysis are incapable of determining the transverse normal stress, this quantity could not be compared. Since the laminate was thin, the finite element analysis results were expected to be in close agreement and did agree well with the results provided by the exact analysis.

This analysis provides the basis for many future investigations. The impact analysis and contact phenomenon can be coupled by incorporating the methods introduced by Singh and Paul (1974). This method is an iterative procedure which simultaneously determines the unknown contact area and loading distribution. In this manner the need for an artificial loading distribution, such as Hertzian loading, is eliminated. With the three-dimensional exact transient solution for the impacted panel, various damage criterion can then be used to evaluate the structural integrity of the laminate.

The most important subject which needs to be addressed in the future is material damping. In the thin laminate analysis, the damping parameter ϵ is treated to be small giving an essentially elastic solution. The sandwich panel analysis, however, contained elastic face sheets laminated to an absorptive core. As demonstrated by the response of the sandwich panel, the stress and displacement fields are highly dependent upon the damping factor. Methods to analyze and describe the damping factor have yet to be determined.

APPENDIX A. AVERAGE MATERIAL CONSTANTS FOR BALANCED LAMINATES

Since only specially orthotropic materials can be examined using the previous formulation, laminates with plies oriented other than 0° or 90° cannot be analyzed. A method exists, however, which determines the average specially orthotropic stiffness matrix for a balanced laminate. A balanced laminate is a panel which for every positively oriented ply there is a negatively oriented ply. For example, for ever +35° ply there is a -35° ply. Thus, this analysis can be expanded to model any balanced laminate if a average stiffness or compliance matrix is determined.

To determine the average stiffness matrix, the stiffness matrix of each ply in the global coordinates is required. The stress-strain relationship for the k^{th} layer of a laminate can be represented as

$$\sigma^k = C^k \epsilon^k \tag{86}$$

or

$$\tilde{\sigma}^k = \tilde{C}^k \tilde{\epsilon}^k \tag{87}$$

where the " ~ " denotes the quantities in the local reference frame. The unit vectors of the local reference frame can be written in terms of the direction cosines and the global unit vectors as

$$\begin{Bmatrix} n_\xi \\ n_\eta \\ n_\zeta \end{Bmatrix}^k = \begin{bmatrix} l_1 & m_1 & n_1 \\ l_2 & m_2 & n_2 \\ l_3 & m_3 & n_3 \end{bmatrix}^k \begin{Bmatrix} n_x \\ n_y \\ n_z \end{Bmatrix} \tag{88}$$

With these direction cosines, stresses and strains can be transformed to the global reference frame through the transformation

$$\begin{aligned} \sigma^k &= T^k \bar{\sigma}^k \\ \epsilon^k &= T^k \bar{\epsilon}^k \end{aligned} \tag{89}$$

where

$$T^k = \begin{bmatrix} l_1^2 & l_2^2 & l_3^2 & 2l_2l_3 & 2l_1l_3 & 2l_1l_2 \\ m_1^2 & m_2^2 & m_3^2 & 2m_2m_3 & 2m_1m_3 & 2m_1m_2 \\ n_1^2 & n_2^2 & n_3^2 & 2n_2n_3 & 2n_1n_3 & 2n_1n_2 \\ m_1n_1 & m_2n_2 & m_3n_3 & (m_2n_3+m_3n_2) & (m_1n_3+m_3n_1) & (m_1n_2+m_2n_1) \\ l_1n_1 & l_2n_2 & l_3n_3 & (l_2n_3+l_3n_2) & (l_1n_3+l_3n_1) & (l_1n_2+l_2n_1) \\ l_1m_1 & l_2m_2 & l_3m_3 & (l_2m_3+l_3m_2) & (l_1m_3+l_3m_1) & (l_1m_2+l_2m_1) \end{bmatrix}^k \tag{90}$$

Substituting equations 88 and 89 into equation 86 while noting

$$T^k T^{k^T} = I \tag{91}$$

yields

$$\sigma^k = T^k \bar{C}^k T^{k^T} \epsilon^k \tag{92}$$

thus the transformation of the stiffness matrix from local coordinates to global coordinates is

$$C^k = T^k \bar{C}^k T^{k^T} \tag{93}$$

The average stiffness matrix (Γ) of a balanced laminate is then represented as

$$\Gamma = \frac{1}{h} \sum_{1}^{n} t^k C^k \tag{94}$$

which represents an average weighting of the stiffness matrix based on the thickness of the layer. Provided the laminate is balanced, Γ will represent a specially orthotropic material with 12 nonzero coefficients, nine of which are independent. This averaging process is expected to provide reasonably acceptable results provided the paired balancing plies are located closely to one another and the plies are relatively thin.

REFERENCES

Ambartsumyan, S.A., 1962, "Contributions to the Theory of Anisotropic Layered Shells," Applied Mechanics Review, Vol. 15, No. 4, pp. 245-249.

Cairns, D.S. and Lagace, P.A., 1970, "Exact Solutions for Rectangular Bidirectional Composites and Sandwich Plates," Journal of Composite Materials, Vol. 4, pp. 20-34.

Chattopadhyay, S., 1977, "Response of Elastic Plates to Impact Including the Effect of Shear Deformation," *in* Proceedings 14th Annual Meeting of the Society of Engineering Science, Inc., edited by Sih, G.C., pp. 127-138.

Dobyns, A.L., 1981, "Analysis of Simply-Supported Orthotropic Plates Subject to Static and Dynamic Loads," AIAA Journal, Vol. 19, No. 5, pp. 642-650.

Dong, S.B., Pister, K.S. and Taylor, R.L., 1970, "On the Theory of Laminated Anisotropic Shells and Plates," Journal of the Aerospace Sciences, Vol. 29, No. 8, pp. 969-975.

Lee, J.D., Du, S. and Liebowitz, H., 1984, "Three-Dimensional Finite Element and Dynamic Analysis of Composite Laminate Subjected to Impact," Computers and Structures, Vol. 19, pp. 807-813.

Lee, L.J., Huang, K.Y. and Fann, Y.J., 1993, "Dynamic Responses of Composite Sandwich Plate Impacted by a Rigid Ball," Journal of Composite Materials, Vol. 27, No. 13, pp. 1238-1256.

Lih, S-S and Mal, A.K., 1995, "Elastic Waves from a Distributed Surface Source in a Unidirectional Composite Laminate," AMD-Vol. 205, pp. 209-219.

Mal, A.K. and Lih, S-S, 1992, "Elastodynamic Response of a Unidirectional Composite Laminate to Concentrated Surface Loads: Part 1," Journal of Applied Mechanics, Vol. 59, pp. 878-892.

Mal, A.K., 1988, "Wave Propagation in Layered Composite Laminates Under Periodic Surface Loads," Wave Motion, Vol. 10, pp. 257-266.

Mindlin, R.D., 1951, "Influence of Rotatory Inertia and Shear on Flexural Motions of Isotropic, Elastic Plates," Journal of Applied Mechanics, Vol. 18, pp. 31-38.

Nettles, A.T., Lance, D.G. and Hodge, A.J., 1990, "An Examination of Impact Damage in Glass/Phenolic and Aluminum Honeycomb Core Composite Panels," NASA Technical Paper 3042.

Noor, A.K. and Burton, S.B., 1990, "Assessment of Computational Models for Multilayered Composite Shells," Applied Mechanics Review, Vol. 43, No. 4, pp. 67-97.

Olsson, R., 1992, "Impact Response of Orthotropic Composite Plates Predicted from a One-Parameter Differential Equation," AIAA Journal, Vol. 30, No. 6, pp. 1587-1596.

Pagano, N.J., 1970, "Exact Solutions for Rectangular Bidirectional Composites and Sandwich Plates," Journal of Composite Materials, Vol. 4, pp. 20-34.

Pister, K.S. and Dong, S.B., 1959, "Elastic Bending of Layered Plates," Journal of the Engineering Mechanics Division, Proceedings of the American Society of Civil Engineers, EM4, pp. 1-10.

Ramkumar, R.L. and Chen, P.C., 1983, "Low-Velocity Impact Response of Laminated Plates," AIAA Journal, Vol. 21, No. 10, pp. 1448-1452.

Reissner, E. and Stavsky, Y., 1961, "Bending and Stretching of Certain Types of Heterogeneous Aeolotropic Elastic Plates," Journal of Applied Mechanics, Vol. 28, pp. 402-408.

Reissner, E., 1950, "On a Variational Theorem in Elasticity," Journal of Mathematics and Physics, Vol. 24, pp. 90-95.

Singh, K.P. and Paul, B., 1974, "Numerical Solution of Non-Hertzian Elastic Contact Problems," Journal of Applied Mechanics, Vol. , pp. 484-490.

Starnes, J.H. Jr. and Williams, J.G., 1984, "Failure Characteristics of Graphite/Epoxy Structural Components Loaded in Compression," NASA TM-84552.

Whitney, J.M. and Sun, C-T, 1977, "Transient Response of Laminated Composite Plates Subjected to Transverse Dynamic Loading," Journal of the Acoustical Society of America, Vol. 61, No. 1, pp. 101-104.

Wu, H-S, T. and Springer, G.S., 1988, "Impact Induced Stresses, Strains, and Delaminations in Composite Plates," Journal of Composite Materials, Vol. 22, pp. 533-560.